JOURNAL OF BACTERIOLOGY, Nov. 2007, p. 7720–7732 Vol. 189, No. 21
0021-9193/07/$08.00+0 doi:10.1128/JB.01081-07

Abh and AbrB Control of *Bacillus subtilis* Antimicrobial Gene Expression▽

Mark A. Strauch,[1]* Benjamin G. Bobay,[2] John Cavanagh,[2] Fude Yao,[1]†
Angelo Wilson,[1] and Yoann Le Breton[1]

Department of Biomedical Sciences, Dental School, University of Maryland, Baltimore, 650 W. Baltimore Street, Baltimore, Maryland 21201,[1] and Department of Molecular and Structural Biochemistry, North Carolina State University, 128 Polk Hall, Raleigh, North Carolina 27695[2]

Received 9 July 2007/Accepted 10 August 2007

The *Bacillus subtilis abh* gene encodes a protein whose N-terminal domain has 74% identity to the DNA-binding domain of the global regulatory protein AbrB. Strains with a mutation in *abh* showed alterations in the production of antimicrobial compounds directed against some other *Bacillus* species and gram-positive microbes. Relative to its wild-type parental strain, the *abh* mutant was found deficient, enhanced, or unaffected for the production of antimicrobial activity. Using *lacZ* fusions, we examined the effects of *abh* upon the expression of 10 promoters known to be regulated by AbrB, including five that transcribe well-characterized antimicrobial functions (SdpC, SkfA, TasA, sublancin, and subtilosin). For an otherwise wild-type background, the results show that Abh plays a negative regulatory role in the expression of four of the promoters, a positive role for the expression of three, and no apparent regulatory role in the expression of the other three promoters. Binding of AbrB and Abh to the promoter regions was examined using DNase I footprinting, and the results revealed significant differences. The transcription of *abh* is not autoregulated, but it is subject to a degree of AbrB-afforded negative regulation. The results indicate that Abh is part of the complex interconnected regulatory system that controls gene expression during the transition from active growth to stationary phase.

Upon entry into stationary phase and sporulation, strains of *Bacillus subtilis* cells produce different spectrums of various antibiotic and antimicrobial functions (36). Among the antimicrobials produced by *B. subtilis* 168 strains are sublancin (27), subtilosin A (2, 35), bacilysocin (46), bacilysin (20, 22, 48), the SdpC sporulation delay toxin (8, 14), the SkfA sporulation killing factor (1, 14), and the TasA protein (37). The pleiotropic AbrB protein is known to play a role in regulating most of these antimicrobials in addition to numerous other genes expressed by postexponential-phase cells (22, 31, 36, 37, 54).

The examination of over 60 chromosomal sites of AbrB binding has failed to uncover a consensus base sequence that has substantive predictive value and that can adequately explain target selection and affinity. High-affinity sites of AbrB-DNA interactions selected using in vitro methods do show convergence to a consensus, but sequences resembling this consensus are rarely found in the chromosomal sites (50, 53). It has been hypothesized that AbrB achieves binding specificity by recognizing three-dimensional DNA architectures that are shared by a finite subset of base sequences (5, 40, 42, 45, 53). A major factor accounting for what has been termed the "limited promiscuity" of AbrB-DNA interactions is believed to be the dynamic flexibility in the DNA-binding domain of the protein; this flexibility allows it to conform to different targets with thermodynamically favorable contacts (4, 6, 47).

B. subtilis contains two AbrB paralogs: Abh (6, 23) and SpoVT (3). The *abh* gene codes for a protein of 92 amino acids, showing 58% overall identity to the AbrB protein. The N-terminal sequence of Abh (first 50 amino acids) shows 74% identity to the N-terminal, DNA-binding region of AbrB. Recently, we determined the nuclear magnetic resonance (NMR) structure of the Abh DNA-binding domain (6) and have begun to examine the DNA-binding properties of intact Abh tetramers. The NMR structure of the Abh DNA-binding domain is remarkably similar to that of AbrB, with most conserved residues having comparable orientations in the putative DNA recognition regions. However, there are subtle structural differences that could contribute to differences in the DNA-binding affinities, DNA-binding specificities, and regulatory scopes of the two proteins.

In order to identify a possible regulatory role for Abh and to ascertain if its regulon overlaps with that of AbrB, we compared *abrB* and *abh* mutant strains for their effects on the production of antimicrobials directed against a variety of *Bacillus* species and other gram-positive bacteria. Using promoter-*lacZ* fusion constructs, we examined the expression of *B. subtilis* antimicrobial-associated operons and observed significant differences between the effects of *abh* versus *abrB* inactivation. We also compared the in vitro abilities of purified Abh and AbrB to bind promoter regions we observed to be subject to both Abh and AbrB regulatory effects in vivo. Our results indicate that Abh is part of the complex interconnected system of regulatory functions that controls gene expression during the transition from active growth to stationary phase, and to our knowledge, our results are the first to identify specific genes regulated by Abh.

MATERIALS AND METHODS

Bacterial strains and plasmids. Plasmids and *Bacillus subtilis* strains used for genetic analysis are listed in Table 1. For simplicity and space considerations, not

* Corresponding author. Mailing address: Department of Biomedical Sciences, Dental School, University of Maryland, Baltimore, 650 W. Baltimore Street, Baltimore, MD 21201. Phone: (410) 706-1815. Fax: (410) 706-0865. E-mail: mstrauch@umaryland.edu.

† Present address: Biotechnology Research Institute, Guangxi Academy of Agricultural Sciences, 44 Daxue Rd. West, Nanning, Guangxi 530007, People's Republic of China.

▽ Published ahead of print on 24 August 2007.

TABLE 1. Plasmids and *B. subtilis* strains[a]

Plasmid or strain	Relevant properties/use	Derivation, source, or reference
Plasmids		
pDG1729	*lacZ* fusions, *thrC* insertion (Sp^r)	P. Stragier
pDH32	*lacZ* fusions, *amyE* insertion, (Cm^r)	J. Hoch
pDR67	p*Spac* fusions, *amyE* insertion, (Cm^r)	A. Grossman
pEG101	*skfA′-lacZ*	R. Losick
pET21b	Protein expression vector	Novagene
pJM103	pUC19 plus *cat* cassette (Cm^r)	M. Perego
pJM115	*lacZ* fusions, *amyE* insertion (Km^r)	M. Perego
pSG35.8	*aprE* promoter clone	J. Hoch
pUC19	*E. coli* cloning	Laboratory stock
pXH23	*sigW* promoter clone	J. Helmann
pAW73	(pDH32) *sboA′-lacZ*	This study (see the text)
pAW74	(pDH32) *sunA′-lacZ*	This study (see the text)
pAW75	(pDH32) *yqxM′-lacZ*	This study (see the text)
pAW77	(pJM103) *sboA* promoter clone	This study (see the text)
pAW78	(pJM103) *sunA* promoter clone	This study (see the text)
pAW79	(pJM103) *yqxM* promoter clone	This study (see the text)
pCT1	(pDH32) *sdpA′-lacZ*	This study (see the text)
pLB6	(pDR67) p*Spac-abh*	This study (see the text)
pLB20	(pDG1729) *sunA′-lacZ*	This study (see the text)
pMAS3155	(pUC19) *abh* promoter region clone	This study (see the text)
pMAS3157	(pUC19) ca. 1-Kb *mreBH′-abh* cloned fragment	This study (see the text)
pMAS3160	(pJM115) *abh′-lacZ*	This study (see the text)
pMAS3161	(pDH32) *abh′-lacZ*	This study (see the text)
pMAS3162	(pJM103) *mreBH′-abh* (vector HincII site removed)	This study (see the text)
pMAS3163	(pMAS3162) Δ *abh*::*kan*	This study (see the text)
B. subtilis strains		
703abrB4	*trpC2 pheAl spo0AΔ204 abrB4*	J. Hoch
ADL380	(PY79) *tasA*::*spc*	A. Driks
BZH73	*trpC2 pheAl* Δ*abh*::*kan* Δ*amyE*::Φ(*pSpac-abh*) Δ*thrC*::Φ(*sunA′-lacZ*)	This study (see the text)
BZH84	*trpC2 pheAl* Δ*abh*::*kan* Δ*abrB*::*tet* Δ*amyE*::Φ(*pSpac-abh*)Δ *thrC*::Φ(*sunA′-lacZ*)	This study (see the text)
EG169	Δ(*skfA-F*)::*tet* Δ *thrC*::Φ(*cotZ′-lacZ*) *erm*	R. Losick
EG407	Δ(*sdpABC*)::*spc*	R. Losick
JH642	*trpC2 pheAl*	J. Hoch
JH703	*trpC2 pheAl spo0AΔ204*	J. Hoch
JH12312	*trpC2 pheAl* Δ*amyE*::Φ(*aprE′-lacZ*)	M. Perego
JH12567	*trpC2 pheAl* Δ*amyE*::Φ(*spo0E′-lacZ*)	M. Perego
JH12600	*trpC2 pheAl* Δ*amyE*::Φ(*abrB′-lacZ*)	M. Perego
JH12607	*trpC2 pheAl abrB*::*cat*	M. Perego
JH642sunA	*trpC2 pheAl sunA*::*kan*	J. Helmann
HB6236	(CU1065) *fosB*::*cat*	J. Helmann
HB7070	(CU1065)::SPβ7063[*sigW′-lacZ*]	J. Helmann
KD891	*trpC2 pheAl* Δ*amyE*::Φ(*rbsR′-lacZ*)	K. Devine
ORB 3148	*trpC2 pheAl sboA*::*neo*	P. Zuber
ORB3153	*trpC2 pheAl albC*::*cat*	P. Zuber
PY79	Prototrophic 168 strain	P. Youngman
SWV118	*trpC2 pheAl* Δ*abh*::*kan*	JH642 plus pMAS3163
SWV119	*trpC2 pheAl* Δ*abrB*::*tet*	Laboratory stock
SWV124	*trpC2 pheAl spo0AΔ204* Δ*abh*::*kan*	JH703 plus pMAS3163
SWV126	*trpC2 pheAl spo0ΔA204* Δ*abrB4 abh*::*kan*	703abrB4 plus pMAS3163
SWV133	*trpC2 pheAl* Δ*abrB*::*tet* Δ*abh*::*kan*	SWV119 plus pMAS3163
SWV150	*trpC2 pheAl* Δ*abrB*::*tet spo0A*::*kan*	Laboratory stock
SWV217	*trpC2 pheAl spo0AΔ204* Δ*abrB*::*tet*	JH703 × SWV119 DNA
SWV231	*trpC2 pheAl spo0AΔ204* Δ*abrB*::*tet* Δ*abh*::*kan*	SWV217 × SWV118 DNA
SWV1163	*trpC2 pheAl* Δ(*skfA-F*)::*tet*	JH642 × EG169 DNA
SWV1164	*trpC2 pheAl* Δ(*sdpABC*)::*spc*	JH642 × EG407 DNA
SWV1173	*trpC2 pheAl* Δ*abh*::*kan* Δ(*skfA-F*)::*tet*	SWV118 × EG169DNA
SWV1174	*trpC2 pheAl* Δ*abh*::*kan* Δ(*sdpABC*)::*spc*	SWV118 × EG407 DNA
SWV1175	*trpC2 pheAl* Δ*abrB*::*tet* Δ(*sdpABC*)::*spc*	SWV119 × EG407 DNA
SWV1176	*trpC2 pheAl* Δ*abrB*::*tet* Δ(*skfA-F*)::*tet*	SWV119 × EG169 DNA
SWV1237	*trpC2 pheAl fosB*::*cat*	JH642 × HB6236 DNA
SWV1238	*trpC2 pheAl tasA*::*spc*	JH642 × ADL380 DNA

[a] For space considerations, not all strains used in the β-galactosidase assays of this study are listed. However, all strains serving as hosts for *lacZ* fusion constructs or as sources of *lacZ* fusion constructs are listed.

all strains used in the β-galactosidase assays of this study are listed. However, all strains serving as hosts for *lacZ* fusion constructs or as sources of *lacZ* fusion constructs are listed. The following strains used in antimicrobial tests were obtained from the Bacillus Genetic Stock Center: 4A2 (*Bacillus thuringiensis* subsp. *thuringiensis*), 4B1 (*B. thuringiensis* subsp. *finitimus*), 4D1 (*B. thuringiensis* subsp. *kurstaki*), 4Q1 (*B. thuringiensis* subsp. *israelensis*), 5A1 (*Bacillus licheniformis*), 6A1 (*Bacillus cereus*), 6A11 (*Bacillus mycoides*), 7A2 (*Bacillus megaterium*), 8A2 (*Bacillus pumilus*), 9A2 (*Geobacillus stearothermophilus*), 11A1 (*Ba-*

cillus atrophaeus), 13A1 (*Bacillus sphaericus*), 14A1 (*B. pumilus* [Biosubtyl]), 16A1 (*Bacillus circulans*), 17A1 (*Bacillus clausii*), 19A1 (*Bacillus fusiformis*), 23A1 (*Bacillus badius*), 24A1 (*Bacillus pycnus*), 25A1 (*Paenibacillus polymyxa*), 26A1 (*Brevibacillus brevis*), 27E3 (*B. subtilis* natto), 50A1 (*Virgibacillus marismortui*), 60A1 (*Bacillus lentus*), 61A1 (*Bacillus coagulans*), 70A1 (*Sporosarcina ureae*), and 80A1 (*Aneurinibacillus aneurinilyticus*). *Bacillus amyloliquefaciens* was obtained from Marta Perego (the Scripps Research Institute, La Jolla, CA), *B. subtilis* W23S^R from Jim Hoch (the Scripps Research Institute, La Jolla, CA), and the Sterne 34F2 vaccine strain of *Bacillus anthracis* from Arthur Aronson (Purdue University). *Staphylococcus aureus* (ATCC 12228), *Staphylococcus epidermidis* (ATCC 35984), *Streptococcus pyogenes* (clinical isolate), and *Listeria monocytogenes* (clinical isolate) were obtained from Mark Shirtliff (University of Maryland, Baltimore, MD). An isolate of *Enterococcus faecalis* was obtained from Allan Delisle (University of Maryland, Baltimore, MD).

Antimicrobial production assays. The basic procedure we used to test for the production (by strain derivatives of *B. subtilis* JH642) of antimicrobial activity directed towards other species (and *B. subtilis* strain variants) entailed spreading a lawn of the organism to be tested for sensitivity on an agar plate suitable for growth of both the lawn and *B. subtilis*, spotting cells of the *B. subtilis* putative producer strains onto the lawn via a toothpick, incubation at a suitable growth temperature for 16 to 18 h, and examination of the plates for the appearance of a zone of clearing of the lawn around the transferred *B. subtilis* colonies. A number of different base media were used for liquid growth of lawn cell cultures and agar plates: Luria-Bertani (LB), Schaeffer's sporulation medium (SM [34]), brain heart infusion (Bacto BHI; Becton-Dickinson), Trypticase soy broth (BBL TSB; Becton-Dickinson), tryptose blood agar base (TBAB; used for agar plates only [Difco]), YT plus 2.5% NaCl (1% tryptone, 0.5% yeast extract, 2.5% NaCl; used for growth of *V. marismortui*), and terrific broth minus glycerol (per liter, 11.8 g peptone, 23.6 g yeast extract, 9.4 g K_2HPO_4, 2.2 g KH_2PO_4). The above media were also tested with and without 0.25% glucose (except for BHI and TSB, whose formulations contain glucose). Not all media produced suitable growth of individual strains to be tested, and not all combinations were tried for each organism. *B. subtilis* strains to be tested for antimicrobial production were grown 16 to 18 h overnight (as patches streaked from initial single colonies) at 37°C on SM agar plates. Lawns of cells were prepared either by direct spreading of overnight cultures (0.15 to 0.3 ml) on the surfaces of the agar plates (allowed to dry before spotted *B. subtilis* cells were applied) or by spreading 0.3 ml overnight culture mixed with 3 ml molten (50°C) top agar (0.7% agar in the appropriate medium matching the agar plate) and allowing the mixture to harden before the *B. subtilis* cell spots were applied. In some cases, the overnight liquid cultures were centrifuged and the cells were resuspended in an equal volume of TM buffer (10 mM Tris [pH 7.5], 1 mM $MgSO_4$) prior to spreading. For those cases where both methods were directly compared for a given target, we did not observe a significant variability due to using washed versus unwashed lawn cells. For assays of the thermophilic organism *G. stearothermophilus*, the organism was first grown on TBAB plates overnight at 53°C and then cells were scraped from the plates, resuspended in TM buffer, and spread as lawns on the assay plates. *B. subtilis* cells were spotted onto these lawns as described above, and the plates were incubated for 7 to 8 h at 37°C (to allow the growth of *B. subtilis*) prior to being shifted to 53°C for overnight incubation and the growth of the *G. stearothermophilus* lawn.

Construction of Δ*abh*::*kan* and *pSpac-abh*. A 1,076-bp DNA fragment containing a portion from the 5′ end of *mreBH*, the entire coding sequence of *abh*, and the intergenic region separating these reading frames was generated from JH642 DNA by using standard PCR techniques. The primers used for amplification annealed at positions −483 to −466 and +560 to +577, relative to the adenosine in the *abh* ATG start codon. The primers each had 8-bp extensions, specifying EcoRI or BamHI sites, respectively. This fragment was ligated into EcoRI-BamHI-digested pUC19, generating pMAS3157. Standard procedures (33) were used for cloning into *Escherichia coli* DH5α (Bethesda Research Laboratories), and plasmid DNA was isolated using the anion-exchange columns of QIAGEN, Inc. pMAS3157 was digested with BamHI, the ends were made blunt via Klenow fill-in, and then the plasmid was digested with EcoRI. The BamHI(blunt)-EcoRI fragment (about 1 kb) was inserted into EcoRI-HincII-cut pJM103 to create pMAS3162. This step was performed in order to ensure that the only HincII site in pMAS3162 was the one located within the *abh* gene. A kanamycin resistance gene from pJM114 (28) was then inserted in the HincII site of pMAS3162 to generate an interrupted *abh* gene in the resultant plasmid, pMAS3163. An *abh* inactivation strain was created by the transformation (17) of JH642 with linearized pMAS3163 and selection for kanamycin resistance. Transformants which had lost the *cat* marker of the plasmid (thus indicating recombination by a double-crossover event occurring in the *abh* sequences flanking the inserted *kan* gene) were obtained and designated SWV118.

Plasmid pLB6, containing an IPTG (isopropyl-β-D-thiogalactopyranoside)-inducible p*Spac-abh* fusion, was constructed by the insertion of a 411-bp DNA fragment (obtained via PCR) into the *amyE* insertional vector pDR67 (21). The insert fragment contained the intact *abh* reading frame flanked by the 68 bp upstream and 67 bp downstream of the open reading frame. The plasmid was transformed into recipient strains with selection for chloramphenicol resistance and screening for absence of amylase activity (see below).

Construction of *lacZ* transcriptional fusions. Single-copy integrational plasmids containing *abh′-lacZ* transcriptional fusions (pMAS3160 and pMAS3161) were constructed as derivatives of the *amyE*-inserting vectors pJM115 and pDH32. PCR was used to produce a 396-bp fragment that contained the intergenic *mreBH-abh* region and EcoRI- and BamHI-digestible ends. The fragment corresponded to positions −321 to +59 relative to the start of the *abh* reading frame. A 400-bp fragment, containing 382 bp spanning the start of the *sdpA* gene and the upstream of the *yvaV* reading frame (endpoint 373 bp upstream of the *sdpA* reading frame to, and including, the first three *sdpA* codons), was obtained via PCR and inserted into pDH32 to produce pCT1. A 398-bp PCR fragment, containing the *sboA* promoter region (positions −338 to +42 relative to the start of the *sboA* reading frame), was inserted into pDH32 to produce pAW73. A 421-bp PCR fragment, containing the *sunA* promoter region (positions −353 to +50 relative to the start of the *sunA* reading frame), was inserted into pDH32 to produce pAW74. The identical fragment was inserted into pDG1729 (15) to produce pLB20. A 348-bp PCR fragment, containing the *yqxM-sipW-tasA* promoter region (positions −322 to +8 relative to the start of the *yqxM* reading frame), was inserted into pDH32 to produce pAW75. (The sequence of any oligonucleotide used in this study is available upon request.) Transcriptional *lacZ* fusions to the *aprE*, *sigW*, *spo0E*, *rbsRKDACB*, *skfABCDEFGH*, and *abrB* operons have been described previously, and information regarding the strains providing the source of chromosomal DNA preparations used in transforming the fusions into other genetic backgrounds is given in Table 1.

Strains containing single copies of *lacZ* fusions inserted at the *amyE* locus were constructed by transformation using the appropriate vector or chromosomal DNA preparation. Amylase activity was checked on Schaeffer agar plates (34) containing 1% corn starch. Strains containing pLB20 were constructed as above, but with confirmation that the recipients were threonine auxotrophs. Strains containing the *sigW′-lacZ* fusion present on the SPβ7063 prophage were constructed using a lysate of HB7070 and standard SPβ transduction techniques. Antibiotic concentrations used in selective plates were 15 μg ml^{-1} tetracycline, 2 μg ml^{-1} kanamycin, 5 μg ml^{-1} chloramphenicol, 7 μg ml^{-1} neomycin, 75 μg ml^{-1} spectinomycin, 1 μg ml^{-1} erythromycin, and 25 μg ml^{-1} lincomycin.

Protein purification. A DNA fragment containing the *B. subtilis abh* reading frame and ribosome binding site was amplified by PCR and inserted into the expression vector pET21b to place the gene under IPTG-inducible control, and the plasmid was transformed into *E. coli* BL21(DE3). One liter LB broth containing 100 μg/ml ampicillin was inoculated with the expression strain and grown at 37°C with vigorous aeration to an optical density at 600 nm of 0.9. IPTG was added to 1 mM, the temperature was lowered to 30°C, and incubation continued for 5 to 6 h. Cells were harvested by centrifugation and resuspended in 10 mM Tris-HCl (pH 8.3 at 4°C), 1 mM EDTA, 10 mM KCl, 1 mM dithiothreitol (DTT), 0.25 μM 4-(2-aminoethyl)-benzenesulfonyl fluoride, and 0.01% Triton X-100. All subsequent steps were performed at 4°C. The cells were sonicated for 20 cycles of 2-min bursts/3-min rests, followed by centrifugation at 17,000 rpm (Beckman JA-20 rotor) for 25 min. The supernatant was saved as the crude extract. Solid ammonium sulfate was added slowly to the crude extract to a final concentration of 40% and allowed to sit for 30 min, followed by centrifugation at 17,000 rpm. The 40% supernatant was dialyzed versus 10 mM Tris-HCl (pH 8.3 at 4°C), 1 mM EDTA, 10 mM KCl, and 1 mM DTT and applied to a Q-Sepharose column (Pharmacia). Abh bound to the column under these conditions and was eluted using a KCl gradient of 125 to 500 mM. The fractions containing Abh were pooled, dialyzed versus the aforementioned buffer, and loaded onto a heparin-agarose (Sigma) column previously equilibrated with identical buffer. The column was eluted using a gradient of 0 to 250 mM KCl, and Abh-containing fractions were pooled. Portions of the purified protein were concentrated using Centriplus YM3 and Centricon YM3 devices (Amicon). The protein was estimated to be greater than 95% pure, as judged by 12% tricine gel electrophoresis. Purified Abh was dialyzed into 10 mM Tris-HCl (pH 8.3 at 4°C), 1 mM EDTA, 10 mM KCl, and 1 mM DTT. Glycerol was added to a 25% final concentration for storage at −80°C.

B. subtilis AbrB was expressed in *E. coli* and purified as described previously (43, 45).

DNA binding assays. DNA fragments used in DNase I footprinting assays were the following: an EcoRI-BamHI fragment of approximately 450 bp (containing the *skfABCDEFGH* promoter region from pEG101) (14); an EcoRI-

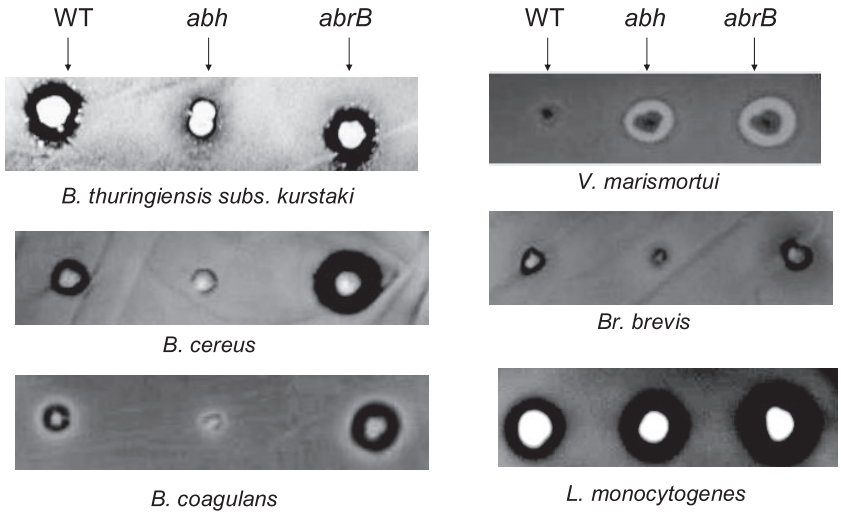

FIG. 1. Differential effects of *abh* and *abrB* mutations upon antimicrobial production directed against select target organisms. The ability of wild-type (WT) (JH642), *abrB*, and *abh* isogenic strains of *B. subtilis* to produce antimicrobial functions against strains of *B. thuringiensis* subsp. *kurstaki*, *B. coagulans*, *B. cereus*, *V. marismortui*, and *L. monocytogenes* under select conditions is depicted. Lawn cells were spread directly onto plates of TBAB (*B. thuringiensis* subsp. *kurstaki*), TBAB plus 0.25% glucose (*B. cereus*, *B. coagulans*, and *B. brevis*), or LB plus 0.25% glucose (*L. monocytogenes*), or lawn cells were mixed with top agar and poured onto YT plus 2.5% NaCl (*V. marismortui*). See the text for further details concerning conditions of the media employed. Isolated colonies of *B. subtilis* wild-type (JH642), *abh* (SWV118), and *abrB* (SWV119) strains were spotted onto the lawns and the plates incubated overnight at 37°C. The different appearance of the lysis zones on the *V. marismortui* plate is due to back illumination (white background), whereas the other photos were taken with overhead illumination (black background).

HindIII fragment of approximately 400 bp (containing the *sdpABC* promoter region from pCT1) (this study); an EcoRI-BamHI fragment of approximately 300 bp (containing the *aprE* promoter region from pSG35.8) (16); a BamHI-HindIII fragment of approximately 160 bp (containing the *sigW* promoter region from pXH23) (19); an EcoRI-BamHI fragment of approximately 400 bp (containing the *abh* promoter region from pMAS3155) (this study); an EcoRI-BamHI fragment of approximately 420 bp (containing the *sunA* promoter from pAW78) (this study); an EcoRI-BamHI fragment of approximately 400 bp (containing the *sboA* promoter from pAW77) (this study); and an EcoRI-BamHI fragment of approximately 350 bp (containing the *yqxM* promoter from pAW79) (this study).

Plasmids containing the fragments were linearized at a unique restriction enzyme site flanking the insert and labeled using [α-^{32}P]dATP (Amersham) and the Klenow enzyme, followed by the inactivation of the Klenow and the release of the singly end-labeled fragment via digestion at a unique site on its opposite flank. Labeled DNA fragments were purified using standard polyacrylamide gel electrophoresis and electroelution techniques. Protein binding buffer composition (1×) was 50 mM Tris (either pH 7 or pH 8), 10 mM $MgCl_2$, 100 mM KCl, 10 mM 2-mercaptoethanol, and 100 μg/ml bovine serum albumin. We have previously determined that optimal Abh binding affinity occurs at pH 7 in vitro, whereas optimal AbrB affinity occurs in a broad plateau from pH 8 to above pH 9.5, with only a slight decrease (about twofold) seen for binding at pH 7 (6). Therefore, we performed the in vitro DNA-binding reactions using AbrB at pH 8 and the Abh reactions at both pH 7 and pH 8. DNase I footprinting assays were performed at room temperature (22°C) and analyzed as described previously (45, 51).

β-Galactosidase assays. Strains to be assayed were grown in SM at 37°C with vigorous aeration and sampled from early logarithmic growth through 4 to 5 h past the transition to stationary phase. Assays were performed as described previously, and activities are reported in Miller units (12, 13, 26). Each strain was assayed on at least three separate occasions. The temporal patterns of β-galactosidase expression, relative to those seen in the wild-type backgrounds, were not significantly different on the separate occasions. For a given sampling time, the quantitative β-galactosidase values for a given strain varied by no more than 25% on the separate days. The results shown in this communication are for "same-day" assays of the indication fusions in the various genetic backgrounds.

RESULTS

Comparison of the effects of Abh and AbrB on antimicrobial production by *B. subtilis*. We tested a variety of *Bacillus* species, close *Bacillus* relatives, and other gram-positive microbes (see Materials and Methods) for differential sensitivity to the presence of wild-type, *abh*, and *abrB* strains of *B. subtilis*. In some cases, we observed that factors related to the growth conditions could result in different sensitivity or resistance responses (qualitatively or quantitatively). The major variability-causing factors were the media used to grow cultures of the target lawn cells, the type of medium used for the agar test plates, and either the presence of 0.25% glucose during growth of the target cells or the presence of 0.25% glucose in the agar plates upon which the lawns were spread. However, for all but a few (i.e., *B. subtilis* NCIB3610, *B. circulans*, *B. clausii*, *S. ureae*, *A. aneurinilyticus*, and *B. fusiformis*) of the organisms screened, we observed at least one set of medium and plating conditions where a colony of an *abrB* mutant strain of *B. subtilis* produced a significant zone of clearing of the surrounding lawn cells. In each case where antimicrobial activity was produced by the *abrB* strain, the activity was greater or equal to that produced by the wild-type parental strain (some examples are shown in Fig. 1) and was not produced by a *spo0A* mutant strain (data not shown). This Spo0A phenotype is likely due to overexpression of *abrB* in *spo0A* strains (38, 55) since it could be suppressed by an *abrB* mutation. We did not observe any instances where an *abh* mutation was able to suppress this Spo0A phenotype (data not shown).

In comparing the antimicrobial activity produced by an *abh* mutant strain relative to that produced by the wild type, we observed specific, reproducible instances where the *abh* strain

either was defective in production relative to the wild type or produced an antimicrobial activity greater than did the wild type (Fig. 1). In each case, an *abrB* mutant produced either as much or significantly more of the activity compared to wild type. Although our assessments are strictly confined to a particular defined set of culture conditions giving reproducible qualitative results, the results indicate that Abh plays a regulatory role in the production of one or more antimicrobial compounds active against other species of bacteria.

Abh and AbrB transcriptional control of antimicrobial operons. We examined the expression of *lacZ* reporter fusions to the promoters of the five genetically best-characterized antimicrobial operons of *B. subtilis* 168 (*sunA*, *sboA-alb*, *yqxM-sipW-tasA*, *sdpABC*, and *skfABCDEFGH*) and the promoter of the *sigW* gene, which encodes an alternate RNA polymerase sigma factor directing the transcription of an antibiosis regulon, including genes specifying antibiotic resistance determinants (8–10). We observed evidence of *abh*-mediated regulation of each of these promoters (Fig. 2). The observed *abh*-mediated effects upon expression of the *sdpABC*, *skfAB CDEFGH*, *sboA*, and *yqxM* promoters are consistent with an interpretation that the Abh protein is a negative regulator of their expression, whereas the observed *abh*-mediated effects upon the expression of the *sigW* and *sunA* promoters are consistent with an interpretation that the Abh protein plays some form of a positive role in regulating their expression.

The *abh* effect on the expression of *sdpABC* was both qualitatively and quantitatively different from the *abrB* effect, with the *abrB* mutation clearly being epistatic to the *abh* mutation (Fig. 2). An additional difference was that an *abh* mutation did not relieve the *spo0A* defect in *sdpABC* expression (data not shown), whereas an *abrB* mutation did.

Expression of the *skfABCDEFGH* operon is strictly dependent upon activation by the Spo0A protein commencing after the onset of stationary phase (14), and neither an *abh* mutation nor an *abrB* mutation could suppress the *spo0A* mutation defect (data not shown). However, in a Spo0A$^+$ background, both an *abh* mutation and an *abrB* mutation led to a significant increase in the level of Spo0A-mediated activation. These results imply that both Abh and AbrB proteins function as negative modulators of *skfABCDEFGH* promoter induction.

The *sboA* promoter was slightly overexpressed in the *abh* strain, and its temporal pattern of expression closely mirrored the wild-type pattern. In contrast, the *abrB* mutation resulted in a significant increase in *sboA* expression during both exponential and stationary phases. A *spo0A* mutation totally prevented the increase during stationary-phase expression (data not shown). An *abrB* mutation, but not an *abh* mutation, was capable of suppressing the *spo0A* effect (data not shown).

AbrB-mediated negative regulation of *sigW* and of some SigW-dependent promoters has been described previously (32). In an otherwise wild-type background, *abh* mutants have an effect opposite from that of *abrB* mutants, primarily during exponential growth (Fig. 2). An *abrB* mutation was epistatic to the *abh* mutation. However, the effects of an *abh* mutation in other genetic backgrounds indicate that the role of Abh in *sigW* expression is more complex. Spo0A mutants result in low levels of *sigW* expression, an effect that can be suppressed by *abrB* mutations (32). An *abh* mutation also partially restored the expression defects due to *spo0A* mutations, but this *abh* effect was significantly less than the *abrB* effect (data not shown). Similar dichotomous effects of an *abh* mutation, dependent upon the nature of the *spo0A* gene, were observed for the *aprE* promoter (see below).

The expression of the *sunA* promoter after the onset of stationary phase was noticeably decreased in an *abh* mutant but at near normal levels in an *abrB* mutant (Fig. 2). We constructed *sunA-lacZ* reporter strains having the *abh* gene under control of the IPTG-inducible p*Spac* promoter. In both the presence and the absence of an intact *abrB* gene, IPTG induction of *abh* expression produced a noticeable increase in expression from the *sunA* promoter (Fig. 3). An activator role of Abh in *sunA* expression is further supported by an examination of the effects of various mutations upon the ability of *B. subtilis* 168 strains to produce an antimicrobial activity directed against *B. coagulans* (Fig. 4).

Close inspection of the inhibition assays (Fig. 4), using *B. coagulans* as a target, reveals an intriguing observation. Surrounding the clear halos produced by *B. subtilis* colonies are rings of more intense turbidity than the background lawn growth. These rings may be interpreted as due to a somewhat more dense growth or accumulation of the lawn cells in these areas. If this is the case, then one possibility is that the *B. subtilis* cells are excreting some type of interspecies pheromone that can lure *B. coagulans* cells to their ultimate demise. An alternative possibility is that lysed *B. coagulans* cells, but not the other species examined (Fig. 1), release nutrients allowing greater growth densities on the periphery of the killing zone.

DNA binding of Abh and AbrB at the *sunA*, *sboA*, *yqxM*, *sdpABC*, *skfABCDEFGH*, and *sigW* promoters. Using DNase I footprinting, we tested to determine whether the *abh* and *abrB* effects on expression of the *lacZ* fusions could be correlated with evidence of in vitro DNA binding of purified Abh and AbrB to the targets and whether significant binding differences would be observed. AbrB binding to the *sunA* promoter resulted in a relatively strong degree of cleavage protection in the region from −178 to −105 bp upstream from the *sunA* reading frame. A much weaker region of potential binding was observed in the vicinity of a putative promoter sequence identified by Paik et al. (27). (The actual promoter for the *sunA* operon has not been determined empirically.) The greatest level of Abh-binding-afforded protection was in a portion of the region of strongest AbrB binding. At the higher concentration of Abh used in the experiment (lane 3), protection was still afforded to the region but it appeared that the Abh interaction was significantly different in that downstream sequences were subject to enhanced DNase I cleavage.

Strongest binding of AbrB to the *sboA* promoter (54) occurred from −100 to −39 with a downstream extension seen at higher concentration (Fig. 5C, lane 1). Abh binding to the fragment resulted in a general degree of cleavage protection along the entire length of the fragment. AbrB bound to two distinct regions in the putative promoter region upstream of the *yqxM* operon (Fig. 5B and 6B). Despite repeated attempts, we did not observe any indication of Abh binding (either protection from or enhancement of DNase I cleavage) with this region.

The results shown for Abh binding to the *sunA* and *sboA* promoter regions are for reactions performed at pH 7 (see Materials and Methods). For these targets (and for *yqxM*) we

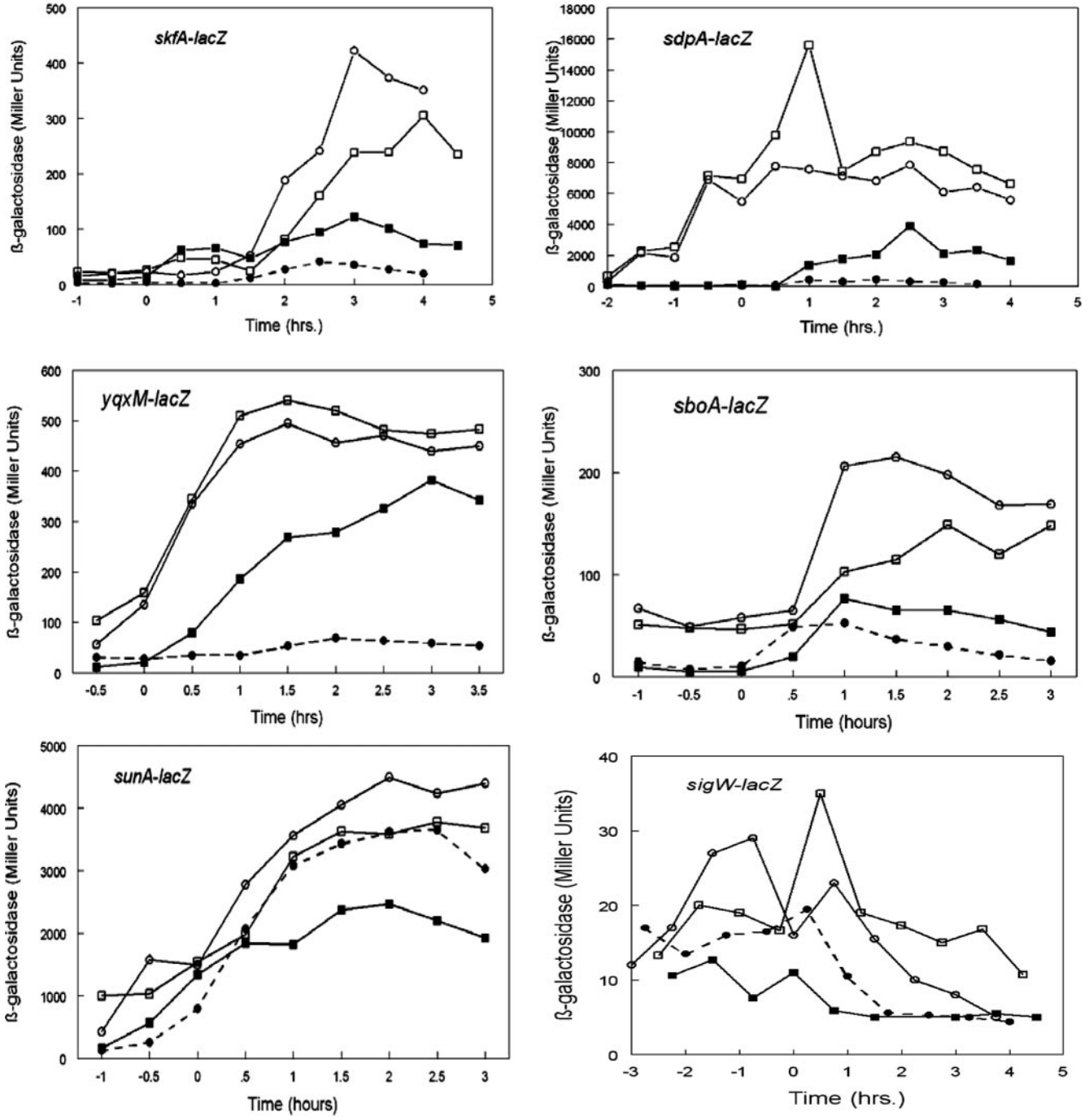

FIG. 2. Differential effects of *abh* and *abrB* mutations upon expression of antimicrobial operon promoters. The expression of *lacZ* transcriptional fusions to the promoters of the *skfA*, *sdpA*, *yqxM*, *sboA*, *sunA*, and *sigW* operons in different genetic backgrounds are shown. Closed circles, wild-type (JH642) background; closed squares, *abh* mutant; open circles, *abrB* mutant; open squares, *abrB abh* mutant. The zeros on the abscissae denote the entry of the cultures into stationary phase.

did not observe a significant effect of pH 8 versus pH 7 on the pattern or extent of the DNase I cleavages due to Abh binding. This was not the case for Abh interactions with the *sdpABC* and *skfABCDEFGH* promoter fragments (Fig. 7).

At pH 8, Abh interaction with the *sdpABC* promoter-containing fragment was manifest primarily as regions of enhanced susceptibility to DNase I (Fig. 7A, left). Our examination of these regions did not reveal any obvious pattern related to helical periodicity or base composition. Abh binding to the *sdpABC* promoter region at pH 7 resulted in extended regions of protection from DNase I that were not obvious when the binding reactions were carried out at pH 8. Some, but not all, of the protected bases seen upon Abh binding at pH 7 are those that showed enhanced susceptibility to DNase I attack

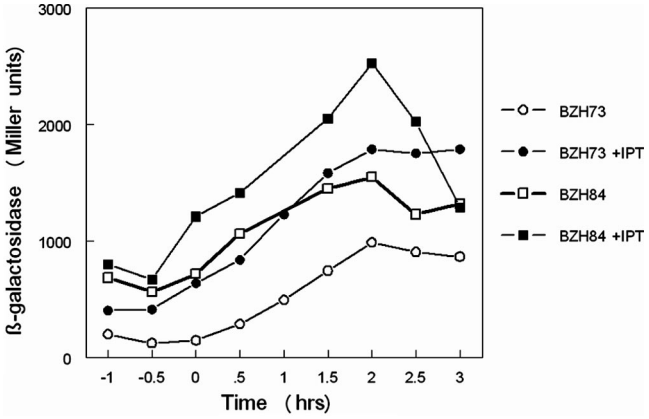

FIG. 3. Induction of *abh* increases *sunA* promoter expression. The time course of β-galactosidase accumulation from a *sunA′-lacZ* fusion in strains carrying an IPTG-inducible p*Spac-abh* construct at the *amyE* locus. Strain BZH73 has a deletion of the native *abh* gene; strain BZH84 is deleted for both the native *abh* and the *abrB* genes. Closed symbols denote cultures having 2 mM IPTG added to the medium at the outset of incubation (approximately 3.5 h before time point 0 on the abscissa, which denotes the entry of the cultures into stationary phase).

when binding was performed at pH 8. These observations imply that Abh interaction with the *sdpABC* promoter region can result in two structurally distinct nucleoprotein complexes in a pH-dependent fashion. This implication contrasts dramatically with the binding behavior of AbrB, which produced essentially identical footprinting patterns on the *sdpABC* region at both pH 7 and pH 8 (AbrB binding at pH 7 not shown).

At pH 7, Abh interaction with the *skfABCDEFGH* promoter region largely resembled that seen at pH 8 (Fig. 7) and was noticeably different from the pattern of AbrB binding. To our knowledge, the location of the promoter(s) responsible for transcription of the *skfABCDEFGH* operon has not been determined, but the extensive nature of AbrB binding in the intergenic region of *ybcM* to *skfA* suggests that AbrB-dependent negative regulation probably entails interference with RNA polymerase binding. The AbrB binding site that overlaps with the perfect Spo0A box presumably required for activation of the *skfABCDEFGH* operon after the onset of stationary phase may play an important fail-safe role that prevents self-immolation or sibling cannibalism at inappropriate times.

AbrB binding to the *sigW* promoter has been reported previously (32). As judged by our DNase I footprinting assays (data not shown), Abh appears to interact only weakly with the *sigW* promoter region. The interactions appear very similar at both pH 7 and pH 8 and are evidenced primarily as weak cleavage protections and enhancements scattered throughout the region.

Abh does not regulate all AbrB-regulated genes. Each of the previously described genes shown to be regulated by Abh are also subject to regulation by AbrB. To determine whether all or only some AbrB-dependent genes are regulated by Abh, we examined the expression of *lacZ* fusions to the promoters of the *aprE* (12), *spo0E* (29, 39), *abrB* (44), and *rbsRKDACB* (41, 49) operons. We did not observe evidence of an Abh role in the regulation of the *spo0E*, *abrB*, and *rbsRKDACB* operons (data not shown). An *abh* mutation did produce a noticeable effect upon the expression of the *aprE* (subtilisin) promoter (Fig. 8).

Interestingly, one known role of subtilisin is in processing the lantibiotic subtilin (11). The AbrB footprint (−60 to +27) seen in Fig. 8 (lane 7) is essentially identical to a previous

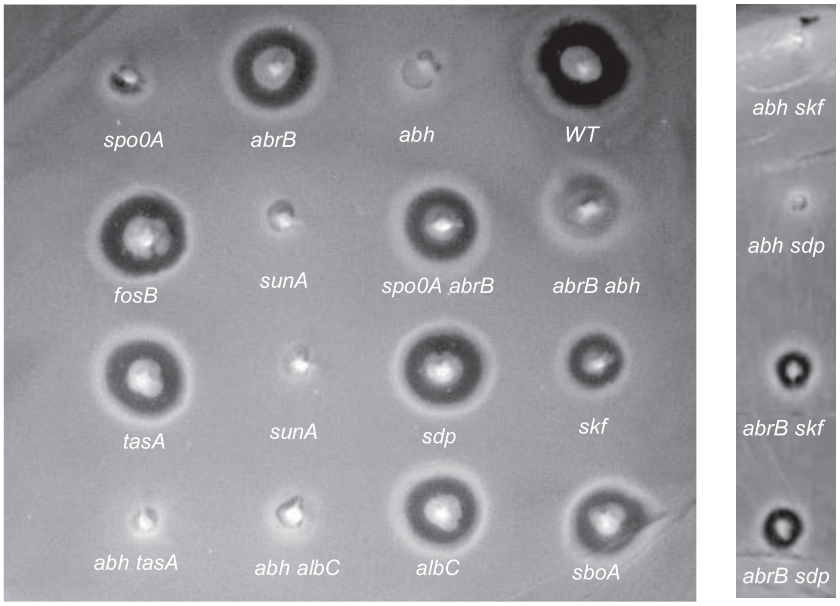

FIG. 4. Production of antimicrobial activity directed against *B. coagulans* by mutant strains of *B. subtilis* 168. The ability of *B. subtilis* mutants to produce antimicrobials against *B. coagulans* is shown. The lawns were spread onto agar plates of TBAB plus 0.25% glucose, which were subsequently incubated at 37°C. The photos shown were taken after approximately 20 h of incubation. Additional incubation times did not affect the general patterns seen, except that the very turbid zone of inhibition surrounding the *abrB abh* cells eventually became clear. WT, wild type.

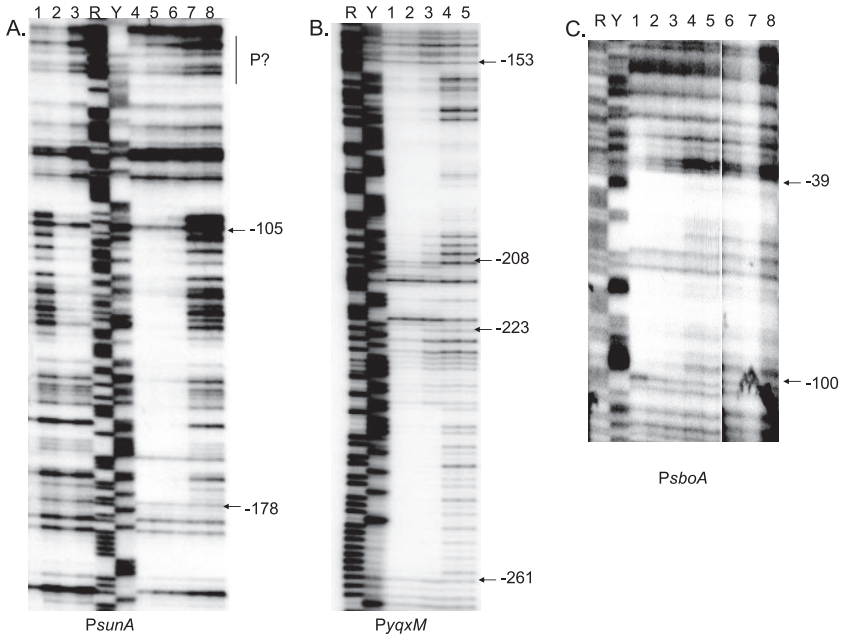

FIG. 5. DNase I footprinting analysis of AbrB and Abh binding to the *sunA*, *yqxM*, and *sboA* promoter regions. (A) Binding to the *sunA* promoter region. Lanes: 1, no protein; 2, 12 μM Abh; 3, 40 μM Abh; 4, 30 μM AbrB; 5, 9 μM AbrB; 6, 3 μM AbrB; 7 and 8, no protein. Binding reactions for lanes 1 to 3 were performed at pH 7; binding reactions for lanes 4 to 8 were performed at pH 8. Maxam-Gilbert purine (R) and pyrimidine (Y) sequence ladders are shown for reference. Base pair positions relative to the beginning of the *sunA* reading frame are indicated to the right; a weaker region of potential binding, denoted by "P?," occurs in the vicinity of a putative promoter sequence identified by Paik et al. (27). (B) Binding to the *yqxM* promoter region. Lanes: 1, 30 μM AbrB; 2, 9 μM AbrB; 3, 3 μM AbrB; 4 and 5, no protein. All binding reactions were performed at pH 8. Base pair positions relative to the beginning of the *yqxM* reading frame are indicated to the right. (C) Binding to the *sboA* promoter region. Lanes: 1, 30 μM AbrB; 2, 9 μM AbrB; 3, 3 μM AbrB; 4 and 5, no protein; 6, 12 μM Abh; 7, 40 μM Abh; 8, no protein. Binding reactions for lanes 1 to 5 were performed at pH 8; binding reactions for lanes 6 to 8 were performed at pH 7. Base pair positions relative to the empirically determined start of transcription (54) are indicated to the right.

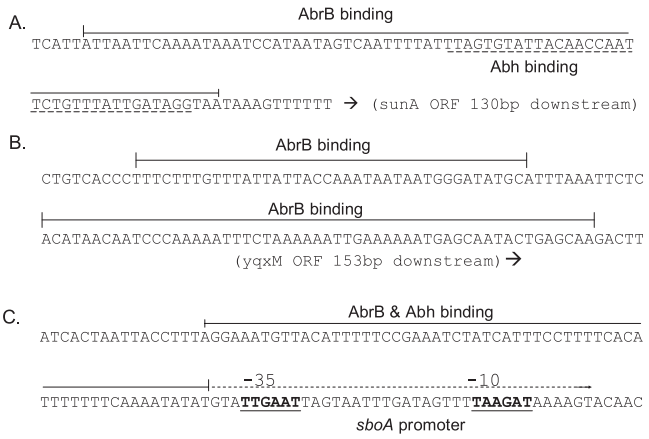

FIG. 6. Locations and sequences of protein binding in the *sunA*, *yqxM*, and *sboA* promoter regions. Empirically determined transcription start points for the *sunA* and *yqxM* promoters have not been published; therefore, the location of the AbrB and Abh binding sites for those regions are indicated relative to the starts of the first protein-coding genes in the operons. The Abh binding region in the *sunA* region is denoted by the dashed line beneath the sequence; all other binding regions are denoted by bracketed lines above the sequences. The dashed line in panel C denotes a region of weaker binding interaction (Fig. 5C); underlined in the panel are *sboA* promoter regions. For clarity, only the nontemplate strands of the binding regions are shown. ORF, open reading frame.

determination (45). An Abh interaction affording cleavage protection from −31 to +28 and resulting in enhanced susceptibility upstream of this region was evident at both pH 7 and pH 8.

AbrB regulates *abh* expression. We constructed an *abh'-lacZ* transcriptional fusion to examine the expression of the *abh* gene (Fig. 9). An *abrB* mutation resulted in an approximately twofold increase in *abh'-lacZ* transcription during late vegetative growth and the early stages of stationary phase and sporulation. The inactivation of *abh* had no effect upon expression of the *abh'-lacZ* reporter, indicating that the gene is not autoregulated. Consistent with regulation by AbrB, the deletion of *spo0A* (which produces an increase in *abrB* expression [30, 38, 55]) lowered *abh'-lacZ* expression, while expression in a *spo0A abrB* strain mirrored that seen in the *abrB* mutant.

We performed DNase I footprinting assays on fragments encompassing the *abh-mreBH* intergenic region. Relatively weak AbrB-binding occurred extensively in this region, but no evidence of Abh binding at either pH 7 or pH 8 was observed (data not shown).

DISCUSSION

The NMR structure of N domain dimers of the *B. subtilis* Abh protein is remarkably similar to the structure of N-terminal DNA-binding domain dimers of its paralog AbrB (6). That the Abh protein is a DNA-binding protein has been shown previously (6), and it is highly probable that the DNA-binding

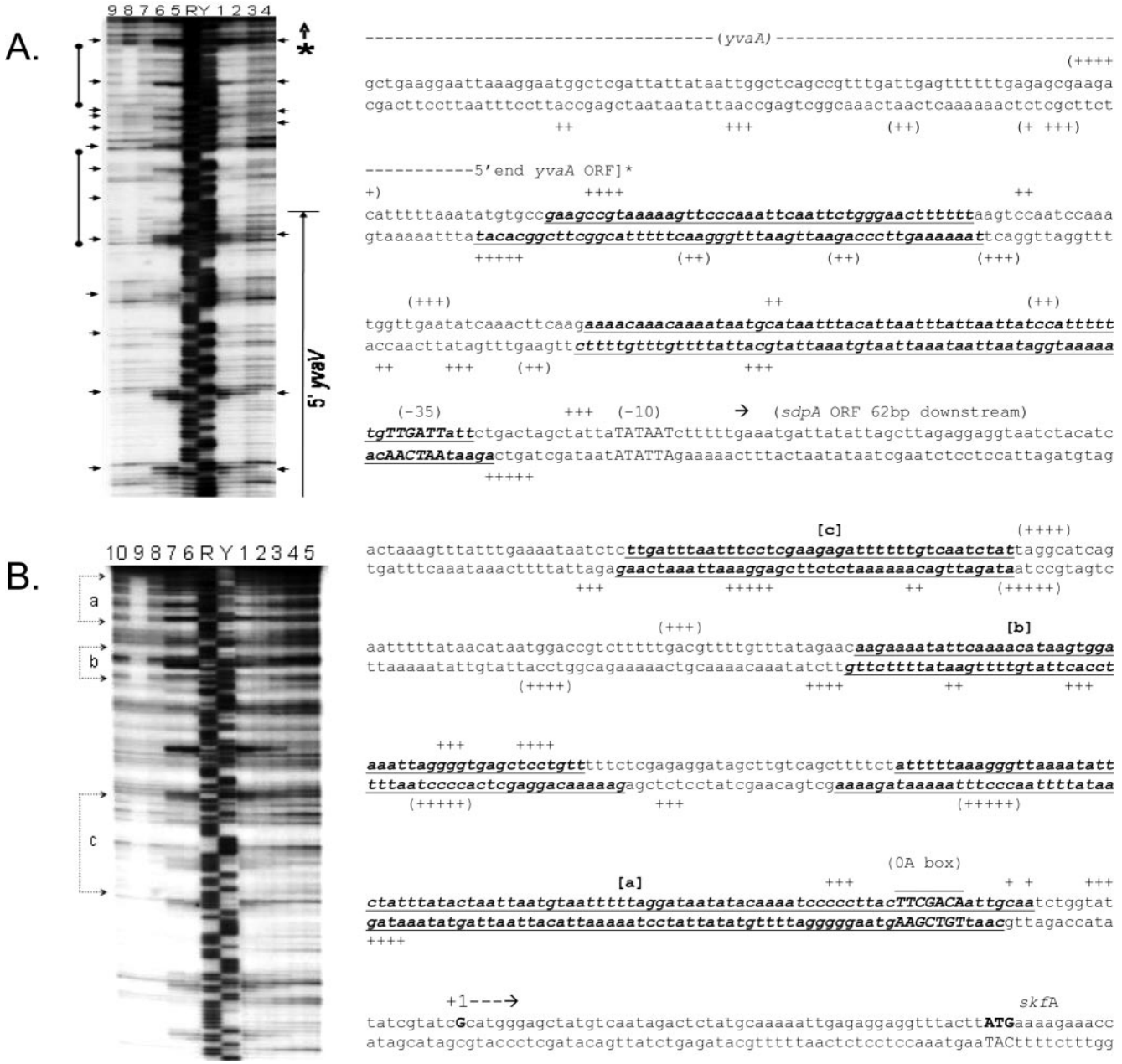

FIG. 7. AbrB and Abh binding to the *sdpABC* and *skfABCDEFGH* promoter regions. (A) (Upper left) DNase I footprinting results of AbrB and Abh binding to a DNA fragment containing the *sdpABC* promoter region. Shown are the results on the template strand (the lower strand shown to the right) labeled at its 3′ end. Lanes 1 to 4 show binding reactions carried out at pH 7; lanes 5 to 9 show reactions carried out at pH 8. Lanes: 1 and 5, 40 μM Abh protein; 2 and 6, 12 μM Abh; 3 and 4 μM Abh; 4, 7, and 9, no binding protein; 8, 10 μM AbrB. Maxam-Gilbert purine (R) and pyrimidine (Y) sequence ladders are used for reference. The asterisk denotes the position of a putative promoter transcribing the *sdp* operon (Fig. 5), and the extents of the 5′ sequences of the *yvaV* gene are shown on the right. The vertical lines on the left denote the approximate extents of the AbrB binding regions visible in lane 8. The horizontal arrows point out regions of enhanced susceptibility to DNaseI attack due to binding of Abh at either pH 7 (arrows on right) or pH 8 (arrows on left). (Upper right) Cartoon depicting results of DNase I footprinting of Abh and AbrB binding to the *sdpABC* promoter region. The 5′ end of the *yvaV* gene and a putative σ^A promoter (−35 and −10 regions in uppercase letters), whose start point (horizontal arrow) would be located about 62 bp upstream of the *sdpA* gene, are indicated for reference. The sequence regions depicted in underlined, bold, italic characters are those bound by AbrB. The plus signs above and below the strand sequences indicate the positions on the corresponding strand that are subject to noticeable sensitivity to DNase I attack in the presence of Abh protein. The plus signs enclosed in parentheses denote positions of Abh-enhanced DNase I sensitivity occurring primarily, or only, at pH 8. Pluses that are not enclosed by parentheses are regions subject to Abh-enhanced DNase I sensitivity at both pH 7 and pH 8. (B) (Lower left) DNase I footprinting results of AbrB and Abh binding to a DNA fragment containing the *skfABCDEFGH* promoter region. Shown are the results on the template strand (the lower strand shown to the right) labeled at its 3′ end. Lanes 1 to 5 show binding reactions carried out at pH 7; lanes 6 to 10 show reactions carried out at pH 8. Lanes: 1 and 6, 40 μM Abh protein; 2 and 7, 12 μM Abh; 3, 4 μM Abh; 4, 5, 8, and 10, no binding protein; 9, 10 μM AbrB. Regions denoted to the left as a, b, and c correspond to the AbrB binding regions, and their sequences are shown to the lower right. (Lower right) Cartoon depicting results of DNase I footprinting of Abh and AbrB binding to the *skfABCDEFGH* promoter region. The

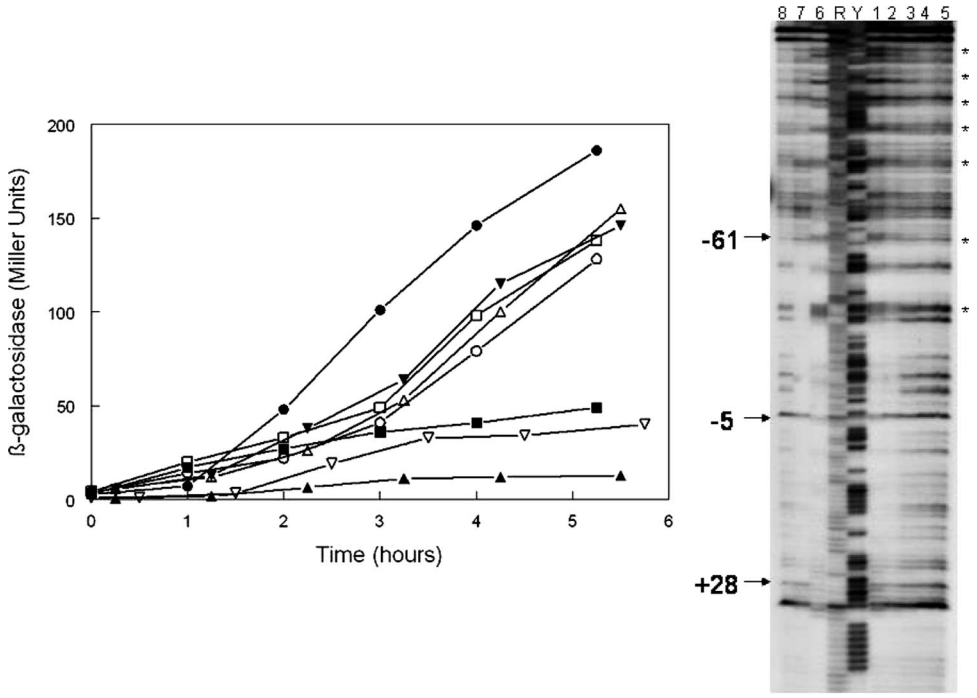

FIG. 8. Regulation of *aprE* expression by *abh*. (Left) Expression of an *aprE′-lacZ* transcriptional fusion in different genetic backgrounds. Closed circles, wild-type background; closed squares, *abh* mutant; closed upright triangles, *spo0A* mutant; closed inverted triangles, *spo0A abrB abh* triple mutant; open circles, *abrB* mutant; open squares, *abrB abh* double mutant; open upright triangles, *spo0A abrB* double mutant; open inverted triangles, *spo0A abh* double mutant. The zero on the abscissa denotes the entry of the cultures into stationary phase. (Right) DNase I footprinting results of AbrB and Abh binding to a DNA fragment containing the *aprE* promoter region. Shown are the results on the nontemplate strand labeled at its 3′ end. Lanes 1 to 5 show binding reactions carried out at pH 7; lanes 6 to 8 show reactions carried out at pH 8. Lanes: 1 and 6, 40 μM Abh protein; 2, 12 μM Abh; 3, 4 μM Abh; 4, 5, and 8, no binding protein; 7, 10 μM AbrB. Maxam-Gilbert purine (R) and pyrimidine (Y) sequence ladders were used for reference. Reference positions relative to the start of transcription are indicated on the left. Asterisks on the right mark areas subject to enhanced DNase I cleavage in the presence of Abh at pH 7, pH 8, or both pHs.

properties of Abh reside primarily in the N-terminal domains of its monomeric subunits. Given the remarkable similarity in the structures of their DNA-binding domains, we have begun to determine whether Abh plays a role in regulating some or all of the same genes controlled by AbrB. One of the best-known and crucial physiological roles played by AbrB is participation in the regulatory control of antibiotics expressed by *B. subtilis* as the cells enter stationary phase. To determine what, if any, role Abh might also play in the expression of these functions, we compared *abh* and *abrB* mutant strains for the total production of antimicrobials active against other species of bacteria, examined the effects of the mutations on the expression of known antibiotic synthesis operons, and compared the in vitro DNA binding properties of the two proteins to the promoter regions of these operons. Our results show that Abh does play a role in regulating the spectrum of antibiotics expressed by *B. subtilis* and that the effects of *abh* and *abrB* mutations differ either qualitatively or quantitatively for each of the shared target promoters whose expression we examined. To our knowledge, this is the first communication to identify specific genes regulated by Abh.

The expression of each of the five antibiotic synthesis operons we have examined has been previously reported to be subject to some form of negative regulation exerted by AbrB (for a review, see reference 36). Our β-galactosidase assays and footprinting studies locating regions of AbrB binding in the promoter regions confirm and extend upon the previous reports. Although an *abrB* mutation had only a modest effect on *sunA* promoter expression under the conditions we examined, it should be noted that the overexpression of AbrB, due to the presence of a *spo0A* mutation, decreases *sunA* expression significantly and *abrB* mutations relieve the *spo0A* effect (data not shown). Such observations indicate that AbrB can function as a repressor of *sunA*. The effects of an *abh* mutation (in an

location(s) of the Spo0A-activated promoter(s) responsible for transcription of the *skfABCDEFGH* operon has not been determined, but the start of the *skfA* reading frame and a 7-bp sequence with perfect homology to a Spo0A recognition box (5′-TGNCGAA-3′) (38) are indicated for reference. The three sequence regions in underlined, bold, italic characters are those bound by AbrB (labeled a, b, and c, corresponding to the regions denoted to the left). The plus signs above and below the strand sequences indicate the positions on the corresponding strand that are subject to noticeable sensitivity to DNase I attack in the presence of Abh protein. The plus signs enclosed in parentheses denote positions of Abh-enhanced DNase I sensitivity occurring primarily, or only, at pH 8. Pluses that are not enclosed by parentheses are regions subject to Abh-enhanced DNase I sensitivity at both pH 7 and pH 8. ORF, open reading frame.

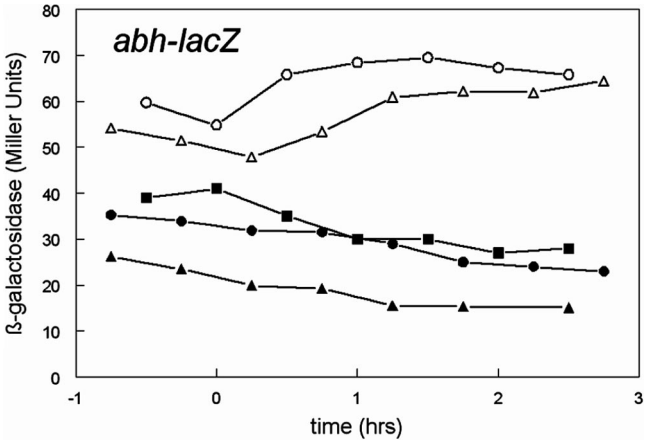

FIG. 9. Regulation of *abh* expression by AbrB. The time course of β-galactosidase accumulation from an *abh'-lacZ* fusion in the following genetic backgrounds: wild type (closed circles), *abrB* (open circles), *abh* (closed squares), *spo0A* (closed triangles), and *spo0A abrB* (open triangles). The zero on the abscissa denotes the entry of the cultures into stationary phase.

otherwise wild-type background) upon the expression of the *sdpABC*, *skfABCDEFGH*, and *yqxM* promoters are consistent with an interpretation that the Abh protein is also a negative regulator of their expression under these conditions. In contrast, Abh appears to act as a positive factor for the expression from the *sunA* promoter during early stationary phase. Abh also seems to play some type of activating role for expression of *aprE* after the onset of stationary phase and a modest activating role for *sigW* expression during late exponential and early stationary phases. In each case where an epistatic relationship could be unambiguously ascertained, *abrB* mutations were epistatic to *abh* mutations.

It is obvious that the DNA binding properties of Abh differ significantly from those of AbrB. Contrasting with the sharply defined extents of AbrB binding interactions evidenced in the DNase I footprinting protection patterns seen here and in numerous prior studies (39–42, 45, 51–53), Abh might have a more relaxed binding specificity and perhaps a greater tendency for cooperative promulgation of binding extension into adjacent DNA regions in a sequence-independent fashion. Nevertheless, as judged by the altered DNase I cleavage patterns we do observe, Abh can interact in vitro with the promoter regions of the *sdpABC*, *skfABCDEFGH*, *sunA*, *sboA*, and *aprE* operons (and perhaps very weakly with the *sigW* promoter). In contrast, we have not observed any evidence of Abh interaction with the *yqxM* promoter. A striking effect of reaction pH can be seen for the Abh-*sdpABC* interaction (Fig. 7); more-subtle pH effects are evident for the interactions with *skfABCDEFGH* and *aprE* (Fig. 7 and 8), but the Abh interactions with the *sunA*, *sboA*, and *sigW* promoters show very little, if any, effect due to pH (Fig. 5 and data not shown). In a separate study (6) employing a synthetic DNA target to which Abh binds with high degree of sequence specificity and gives a sharply delineated region of protection from DNase I cleavage, we determined that optimum Abh binding occurred at pH 7. Abh binding affinity at pH 8 was approximately 5 to 10 times less than at pH 7. The footprinting results shown in Fig. 7 imply that pH also may affect the structure of the nucleoprotein complex formed between Abh and some DNA targets. An intriguing possibility is that the differential binding properties of Abh at pH 8 versus pH 7 might be related to the adaptation to environmental pH (which has been shown to affect *Bacillus* intracellular pH [7, 18]) or to a physiological change in intracellular pH that occurs during the sporulation process (24, 25). One role for Abh may involve assuming or augmenting AbrB repressive effects under conditions leading to lowered intracellular pH. We are currently attempting to assess the potential physiological consequences of Abh's pH preference.

We cannot say with absolute certainty that the DNA binding interactions of Abh we have observed in vitro can be completely correlated with the *abh* effects on promoter expression seen in our β-galactosidase assays, although such a scenario seems probable in many cases. Given that we could not detect evidence of an Abh-*yqxM* binding interaction in vitro, Abh-dependent regulation of the *yqxM* promoter would appear to be one case where the Abh effect is indirect through other, unidentified regulatory factors. But at promoters where Abh and AbrB are capable of binding under identical conditions, the possibility exists that Abh plays a role in displacing, tempering, or augmenting AbrB repressive effects. It might accomplish either of the latter two possibilities by interaction with DNA sequences either within or flanking AbrB binding targets, thereby changing the DNA conformation such that it is presented as either a better or a worse substrate for AbrB interaction. In those cases where in vivo results indicate that an *abrB* mutation is epistatic to an *abh* mutation, the observations are consistent with, but do not prove, a model where the role of Abh is in affecting the AbrB-dependent regulatory mechanism. In this model, the relative levels of AbrB and Abh activity present in the cell under varying environmental and physiological conditions could be a crucial factor determining the extent of expression from the target promoters. The results we have presented concerning the expression of *sunA* and protein binding to the *sunA* promoter region may be used to illustrate such a model. Abh binding to the *sunA* promoter region may function to hinder AbrB interactions in the region. In the absence of Abh, or when AbrB is present at higher intracellular levels (such as in *spo0A* strains), AbrB binding to *sunA* is unimpeded and leads to lowered *sunA* expression. Our attempts to gain additional support of such a model using competitive binding assays have been hampered by the fact that AbrB shows a significantly greater binding affinity than Abh does (on a molar basis) under the variety of in vitro binding conditions we have examined. Of course, it is also difficult to assess the physiological relevance of any such in vitro experimental results without knowledge of how the in vitro assay system actually mimics the specific intracellular environment and possible DNA conformations assumed by the promoter regions in their native chromosomal context.

Another possibility for AbrB-Abh regulatory interactions at some promoters is that Abh and AbrB can form mixed multimers that have DNA-binding properties different from those of the homotetramers. Heterotetramers containing wild-type and mutant AbrB subunits can be formed in vitro (47). We have preliminary evidence that subunit mixing can occur between Abh and AbrB subunits in vitro and that AbrB-Abh interactions can occur in a yeast cell two-hybrid system (E.

Adeishvili and M. A. Strauch, unpublished data), and we have begun to further explore the possible significance of these observations.

Although we do not yet know the entire scope of the Abh regulon, the evidence we have presented indicates that it includes functions involved in the production of, and resistance to, antimicrobials. As such, it overlaps partially with the AbrB regulon. Also evident is that AbrB and Abh can play different regulatory roles at shared target promoters and that these regulatory interactions at any given target might be multifaceted and complex. Experiments are under way to further define the scopes of the Abh and AbrB regulons under different growth and environmental conditions and to explore the interactions between AbrB and Abh that are used by the cell to tailor changes in gene expression to fit the precise challenges to survival that it encounters.

ACKNOWLEDGMENTS

This work was supported in part by National Institutes of Health, U.S. Public Health Service grants GM46700 (M.A.S.) and GM55769 (J.C.).

We thank John Helmann for communicating unpublished results and for helpful discussions; Rich Losick for providing numerous strains, information, and advice regarding the use and properties of the *sdp* and *skf* operons; and Chun Tan for assistance in performing some of the β-galactosidase assays.

REFERENCES

1. **Allenby, N. E., C. A. Watts, G. Homuth, Z. Pragai, A. Wipat, A. C. Ward, and C. R. Harwood.** 2006. Phosphate starvation induces the sporulation killing factor of *Bacillus subtilis*. J. Bacteriol. **188:**5299–5303.
2. **Babasaki, K., T. Takao, Y. Shimonishi, and K. Kurahashi.** 1985. Subtilosin A, a new antibiotic peptide produced by *Bacillus subtilis* 168: isolation, structural analysis, and biogenesis. J. Biochem. **98:**585–603.
3. **Bagyan, I., J. Hobot, and S. Cutting.** 1996. A compartmentalized regulator of developmental gene expression in *Bacillus subtilis*. J. Bacteriol. **178:**4500–4507.
4. **Bobay, B. G., A. Andreeva, G. A. Mueller, J. Cavanagh, and A. G. Murzin.** 2005. Revised structure of the AbrB N-terminal domain unifies a diverse superfamily of putative DNA-binding proteins. FEBS Lett. **579:**5669–5674.
5. **Bobay, B. G., L. Benson, S. Naylor, B. Feeney, A. C. Clark, M. B. Goshe, M. A. Strauch, R. Thompson, and J. Cavanagh.** 2004. Evaluation of the DNA binding tendencies of the transition state regulator AbrB. Biochemistry **43:**16106–16118.
6. **Bobay, B. G., G. A. Mueller, R. J. Thompson, A. G. Murzin, R. A. Venters, M. A. Strauch, and J. Cavanagh.** 2006. NMR structure of AbhN and comparison with AbrBN: first insights into the DNA binding promiscuity and specificity of AbrB-like transition state regulator proteins. J. Biol. Chem. **281:**21399–21409.
7. **Breeuwer, P., J. L. Drocourt, F. M. Rombouts, and T. Abee.** 1996. A novel method for continuous determination of the intracellular pH in bacteria with the internally conjugated fluorescent probe 5 (and 6-)-carboxyfluorescein succinimidyl ester. Appl. Environ. Microbiol. **62:**178–183.
8. **Butcher, B. G., and J. D. Helmann.** 2006. Identification of *Bacillus subtilis* sigma-dependent genes that provide intrinsic resistance to antimicrobial compounds produced by bacilli. Mol. Microbiol. **60:**765–782.
9. **Cao, M., P. A. Kobel, M. M. Morshedi, M. F. Wu, C. Paddon, and J. D. Helmann.** 2002. Defining the *Bacillus subtilis* sigma(W) regulon: a comparative analysis of promoter consensus search, run-off transcription/macroarray analysis (ROMA), and transcriptional profiling approaches. J. Mol. Biol. **316:**443–457.
10. **Cao, M., T. Wang, R. Ye, and J. D. Helmann.** 2002. Antibiotics that inhibit cell wall biosynthesis induce expression of the *Bacillus subtilis* sigma(W) and sigma(M) regulons. Mol. Microbiol. **45:**1267–1276.
11. **Corvey, C., T. Stein, S. Dusterhus, M. Karas, and K. D. Entian.** 2003. Activation of subtilin precursors by *Bacillus subtilis* extracellular serine proteases subtilisin (AprE), WprA, and Vpr. Biochem. Biophys. Res. Commun. **304:**48–54.
12. **Ferrari, E., D. J. Henner, M. Perego, and J. A. Hoch.** 1988. Transcription of *Bacillus subtilis* subtilisin and expression of subtilisin in sporulation mutants. J. Bacteriol. **170:**289–295.
13. **Ferrari, E., S. M. Howard, and J. A. Hoch.** 1986. Effect of stage 0 sporulation mutations on subtilisin expression. J. Bacteriol. **166:**173–179.
14. **González-Pastor, J. E., E. C. Hobbs, and R. Losick.** 2003. Cannibalism by sporulating bacteria. Science **301:**510–513.
15. **Guérout-Fleury, A. M., N. Frandsen, and P. Stragier.** 1996. Plasmids for ectopic integration in *Bacillus subtilis*. Gene **180:**57–61.
16. **Henner, D. J., E. Ferrari, M. Perego, and J. A. Hoch.** 1988. Location of the targets of the *hpr-97*, *sacU32*(Hy), and *sacQ36*(Hy) mutations in upstream regions of the subtilisin promoter. J. Bacteriol. **170:**296–300.
17. **Hoch, J. A.** 1991. Genetic analysis in *Bacillus subtilis*. Methods Enzymol. **204:**305–320.
18. **Hornbaek, T., M. Jakobsen, J. Dynesen, and A. K. Nielsen.** 2004. Global transcription profiles and intracellular pH regulation measured in *Bacillus licheniformis* upon external pH upshifts. Arch. Microbiol. **182:**467–474.
19. **Huang, X., and J. D. Helmann.** 1998. Identification of target promoters for the *Bacillus subtilis* sigma X factor using a consensus-directed search. J. Mol. Biol. **279:**165–173.
20. **Inaoka, T., K. Takahashi, M. Ohnishi-Kameyama, M. Yoshida, and K. Ochi.** 2003. Guanine nucleotides guanosine 5′-diphosphate 3′-diphosphate and GTP co-operatively regulate the production of an antibiotic bacilysin in *Bacillus subtilis*. J. Biol. Chem. **278:**2169–2176.
21. **Ireton, K., D. Z. Rudner, K. J. Siranosian, and A. D. Grossman.** 1993. Integration of multiple developmental signals in *Bacillus subtilis* through the Spo0A transcription factor. Genes Dev. **7:**283–294.
22. **Karataçs, A. Y., S. Cetin, and G. Ozcengiz.** 2003. The effects of insertional mutations in *comQ*, *comP*, *srfA*, *spo0H*, *spo0A* and *abrB* genes on bacilysin biosynthesis in *Bacillus subtilis*. Biochim. Biophys. Acta **1626:**51–56.
23. **Kobayashi, K., K. Shoji, T. Shimizu, K. Nakano, T. Sato, and Y. Kobayashi.** 1995. Analysis of a suppressor mutation *ssb* (*kinC*) of *sur0B20* (*spo0A*) mutation in *Bacillus subtilis* reveals that *kinC* encodes a histidine protein kinase. J. Bacteriol. **177:**176–182.
24. **Magill, N. G., A. E. Cowan, D. E. Koppel, and P. Setlow.** 1994. The internal pH of the forespore compartment of *Bacillus megaterium* decreases by about 1 pH unit during sporulation. J. Bacteriol. **176:**2252–2258.
25. **Magill, N. G., A. E. Cowan, M. A. Leyva-Vazquez, M. Brown, D. E. Koppel, and P. Setlow.** 1996. Analysis of the relationship between the decrease in pH and accumulation of 3-phosphoglyceric acid in developing forespores of *Bacillus* species. J. Bacteriol. **178:**2204–2210.
26. **Miller, J. H.** 1972. Experiments in molecular genetics. Cold Spring Harbor Laboratory Press, Cold Spring Harbor, NY.
27. **Paik, S. H., A. Chakicherla, and J. N. Hansen.** 1998. Identification and characterization of the structural and transporter genes for, and the chemical and biological properties of, sublancin 168, a novel lantibiotic produced by *Bacillus subtilis* 168. J. Biol. Chem. **273:**23134–23142.
28. **Perego, M.** 1993. Integrational vectors for genetic manipulation in *Bacillus subtilis*, p. 615–624. *In* A. L. Sonenshein, J. A. Hoch, and R. Losick (ed.), *Bacillus subtilis* and other gram-positive bacteria: biochemistry, physiology, and molecular genetics. American Society for Microbiology, Washington, DC.
29. **Perego, M., and J. A. Hoch.** 1991. Negative regulation of *Bacillus subtilis* sporulation by the *spo0E* gene product. J. Bacteriol. **173:**2514–2520.
30. **Perego, M., G. B. Spiegelman, and J. A. Hoch.** 1988. Structure of the gene for the transition state regulator, *abrB*: regulator synthesis is controlled by the *spo0A* sporulation gene in *Bacillus subtilis*. Mol. Microbiol. **2:**689–699.
31. **Phillips, Z. E., and M. A. Strauch.** 2002. *Bacillus subtilis* sporulation and stationary phase gene expression. Cell. Mol. Life Sci. **59:**392–402.
32. **Qian, Q., C. Y. Lee, J. D. Helmann, and M. A. Strauch.** 2002. AbrB is a regulator of the sigma(W) regulon in *Bacillus subtilis*. FEMS Microbiol. Lett. **211:**219–223.
33. **Sambrook, J., and D. Russell.** 2001. Molecular cloning: a laboratory manual, 3rd ed. Cold Spring Harbor Laboratory Press, Cold Spring Harbor, NY.
34. **Schaeffer, P., J. Miller, and J. Aubert.** 1965. Catabolite repression of bacterial spoulation. Proc. Natl. Acad. Sci. USA **54:**701–711.
35. **Shelburne, C. E., F. Y. An, V. Dholpe, A. Ramamoorthy, D. E. Lopatin, and M. S. Lantz.** 2007. The spectrum of antimicrobial activity of the bacteriocin subtilosin A. J. Antimicrob. Chemother. **59:**297–300.
36. **Stein, T.** 2005. *Bacillus subtilis* antibiotics: structures, syntheses and specific functions. Mol. Microbiol. **56:**845–857.
37. **Stöver, A. G., and A. Driks.** 1999. Regulation of synthesis of the *Bacillus subtilis* transition-phase, spore-associated antibacterial protein TasA. J. Bacteriol. **181:**5476–5481.
38. **Strauch, M., V. Webb, G. Spiegelman, and J. A. Hoch.** 1990. The SpoOA protein of *Bacillus subtilis* is a repressor of the *abrB* gene. Proc. Natl. Acad. Sci. USA **87:**1801–1805.
39. **Strauch, M. A.** 1996. Dissection of the *Bacillus subtilis spo0E* binding site for the global regulator AbrB reveals smaller recognition elements. Mol. Gen. Genet. **250:**742–749.
40. **Strauch, M. A.** 1995. In vitro binding affinity of the *Bacillus subtilis* AbrB protein to six different DNA target regions. J. Bacteriol. **177:**4532–4536.
41. **Strauch, M. A.** 1995. AbrB modulates expression and catabolite repression of a *Bacillus subtilis* ribose transport operon. J. Bacteriol. **177:**6727–6731.
42. **Strauch, M. A.** 1995. Delineation of AbrB-binding sites on the *Bacillus subtilis spo0H*, *kinB*, *ftsAZ*, and *pbpE* promoters and use of a derived

homology to identify a previously unsuspected binding site in the *bsuB1* methylase promote. J. Bacteriol. **177:**6999–7002.
43. **Strauch, M. A., P. Ballar, A. J. Rowshan, and K. L. Zoller.** 2005. The DNA-binding specificity of the *Bacillus anthracis* AbrB protein. Microbiology **151:**1751–1759.
44. **Strauch, M. A., M. Perego, D. Burbulys, and J. A. Hoch.** 1989. The transition state transcription regulator AbrB of *Bacillus subtilis* is autoregulated during vegetative growth. Mol. Microbiol. **3:**1203–1209.
45. **Strauch, M. A., G. B. Spiegelman, M. Perego, W. C. Johnson, D. Burbulys, and J. A. Hoch.** 1989. The transition state transcription regulator AbrB of *Bacillus subtilis* is a DNA binding protein. EMBO J. **8:**1615–1621.
46. **Tamehiro, N., Y. Okamoto-Hosoya, S. Okamoto, M. Ubukata, M. Hamada, H. Naganawa, and K. Ochi.** 2002. Bacilysocin, a novel phospholipid antibiotic produced by *Bacillus subtilis* 168. Antimicrob. Agents Chemother. **46:** 315–320.
47. **Vaughn, J. L., V. Feher, S. Naylor, M. A. Strauch, and J. Cavanagh.** 2000. Novel DNA binding domain and genetic regulation model of *Bacillus subtilis* transition state regulator AbrB. Nat. Struct. Biol. **7:**1139–1146.
48. **Walker, J. E., and E. P. Abraham.** 1970. The structure of bacilysin and other products of *Bacillus subtilis*. Biochem. J. **118:**563–570.
49. **Woodson, K., and K. M. Devine.** 1994. Analysis of a ribose transport operon from *Bacillus subtilis*. Microbiology **140:**1829–1838.
50. **Xu, K., D. Clark, and M. A. Strauch.** 1996. Analysis of *abrB* mutations, mutant proteins, and why *abrB* does not utilize a perfect consensus in the −35 region of its sigma A promoter. J. Biol. Chem. **271:**2621–2626.
51. **Xu, K., and M. A. Strauch.** 2001. DNA-binding activity of amino-terminal domains of the *Bacillus subtilis* AbrB protein. J. Bacteriol. **183:**4094–4098.
52. **Xu, K., and M. A. Strauch.** 1996. Identification, sequence, and expression of the gene encoding γ-glutamyltranspeptidase in *Bacillus subtilis*. J. Bacteriol. **178:**4319–4322.
53. **Xu, K., and M. A. Strauch.** 1996. In vitro selection of optimal AbrB-binding sites: comparison to known in vivo sites indicates flexibility in AbrB binding and recognition of three-dimensional DNA structures. Mol. Microbiol. **19:** 145–158.
54. **Zheng, G., L. Z. Yan, J. C. Vederas, and P. Zuber.** 1999. Genes of the *sbo-alb* locus of *Bacillus subtilis* are required for production of the antilisterial bacteriocin subtilosin. J. Bacteriol. **181:**7346–7355.
55. **Zuber, P., and R. Losick.** 1987. Role of AbrB in Spo0A- and Spo0B-dependent utilization of a sporulation promoter in *Bacillus subtilis*. J. Bacteriol. **169:**2223–2230.